UNIVERSITY OF CALIFORNIA

Santa Barbara

Earth Science Department

Brucite-Inspired Ocean Alkalinity Enhancement: Chalking up the Growth and Calcification of *Emiliania huxleyi*

A Senior Thesis submitted in partial satisfaction of the criteria for graduation with Distinction in the Major

by

Angela Grace Larson

Advised by:

Dr. Débora Iglesias-Rodriguez

Dr. Morgan Raven

June 2025

Abstract

Carbon dioxide removal (CDR) has become an increasingly essential area of research in the effort to limit global warming to 2°C above pre-industrial temperature levels–a goal set by the 2015 Paris Agreement. Ocean Alkalinity Enhancement (OAE) is a marine CDR method that aims to capture carbon dioxide (CO_2) by adding alkaline solutions to the surface ocean. Alkalinity additions convert aqueous CO_2 to stable bicarbonate and carbonate ions, causing a surface-ocean CO_2 deficit to be equilibrated by the in-gassing of atmospheric CO_2. OAE shows significant potential for carbon removal, yet critical knowledge gaps persist in understanding the response of marine organisms to the rapid shift in pH and speciation of dissolved inorganic carbon ions from added alkalinity. In a study, we conducted a laboratory mesocosm experiment investigating the impacts of a brucite-inspired alkalinity addition (BIAA) for OAE on the growth and calcification in *Emiliania huxleyi*, a calcareous marine phytoplankton. The treatment used $MgCl_2 * 6H_2O$ and NaOH to raise alkalinity by ~690 μmol kg^{-1}, resulting in a total alkalinity of ~2900 μmol kg^{-1}.

Our results suggest BIAA enhanced the growth rates of *E. huxleyi*, suggesting a possible stimulatory effect of increased magnesium concentrations within seawater. Calcification, measured as cellular particulate inorganic carbon (PIC), remained stable across treatments; however, the PIC:POC (PIC: particulate organic carbon) ratio was significantly higher in BIAA. This is likely a result of reduced POC production within BIAA compared to the Control. Furthermore, the presence of an orange precipitate coincided with the removal of dissolved inorganic phosphate indicates potential nutrient removal in our cultures. Our results further our understanding of the impacts of a magnesium-rich alkalinity addition on the biogeochemical and physiological processes of *E. huxleyi*.

Acknowledgements

First, I would like to thank the Department of Energy and Carbon to the Sea Initiative for funding this research project. Additionally, thank you to the Field-based Undergraduate Engagement through Research, Teaching, and Education (FUERTE) fellowship for personally funding me for the past three years, I am so grateful to have had the opportunity to grow as a researcher and mentor under this fellowship.

I would like to thank my advisors, Dr. Débora Iglesias-Rodriguez and Dr. Morgan Raven, for all the support, guidance, and encouragement. I would also like to thank my partner in crime (or rather, lab), Maddie Manzagol, for her love, support, and camaraderie through heinous lab hours, late-night troubleshooting, and moments of both chaos and laughter that kept me going.

I would also like to recognize Zoë Welch and James Gately for their invaluable guidance in developing and carrying out this project. Through the many long meetings and panicked phone calls, they were always there to assist us and calm our worries. Their advice continues to shape me as a student and early career scientist, and I am forever grateful for all their support.

Additionally, I would like to thank Christoph Pierre at MSI for seawater collection, Ken Marchus at MSI for CHN analysis, David Lyons at UCR for ICP-OES analysis, and UCSD Scripps Analytical Facility for nutrient analysis.

Furthermore, thank you to Jacob Rodriguez, Law Wu, and Elora Shaw for faithfully delivering sustenance and caffeine to the dungeon (our beloved basement lab) throughout the course of the experiment. Special thanks to Coldplay, Charli XCX, and the Glee cast albums for providing the soundtrack not only to our lab work, but also to the writing process—keeping both the spirit and data flowing.

Finally, thank you to my amazing mom, Laura Larson. She has been my number one supporter over these past four years (and the past twenty-two years as well), and I would not have been able to achieve all that I have without her by my side. Thank you, Mom, for everything that you have sacrificed for me and our family. You are the parent that always shows up and I am eternally grateful for everything you do to support me.

Table of Contents

Abstract…….…….. 1
Acknowledgements…….. 2

1. INTRODUCTION……...……...…….. 4

2. METHODS……...……..… 9

2.1. EXPERIMENTAL DESIGN…… 9

2.2. SAMPLE ANALYSES…….. 10
2.2.1. CARBONATE CHEMISTRY…….. 10
2.2.2. PARTICULATE INORGANIC CARBON……... 11
2.2.3. PARTICULATE ORGANIC CARBON AND PARTICULATE ORGANIC NITROGEN…… 11
2.2.4. DISSOLVED INORGANIC NUTRIENTS…….. 11
2.2.5. MICROSCOPY…….. 11
2.2.5. STATISTICAL ANALYSES…… 12

3. RESULTS……...……..…… 12

4. DISCUSSION……...……..…….. 17

5. CONCLUSION……...…….…… 20

6. REFERNCES……...…….……... 22

1. Introduction

Reducing atmospheric carbon dioxide (CO_2) emissions in an effort to limit global average temperature increase below 2°C of pre-industrial temperatures, as stated in the 2015 Paris Agreement (UNFCCC, 2015), is one of the greatest anthropogenic challenges facing humanity today. However, as emissions have continued to rise (Friedlingstein *et al*., 2023), it has become increasingly apparent that this goal will not be achieved without the coupling of emissions reduction and geoengineering approaches for existing atmospheric CO_2. Such approaches that aim to do so are commonly referred to as negative emission technologies or carbon dioxide removal (CDR) (National Academies of Sciences Engineering and Medicine, 2022).

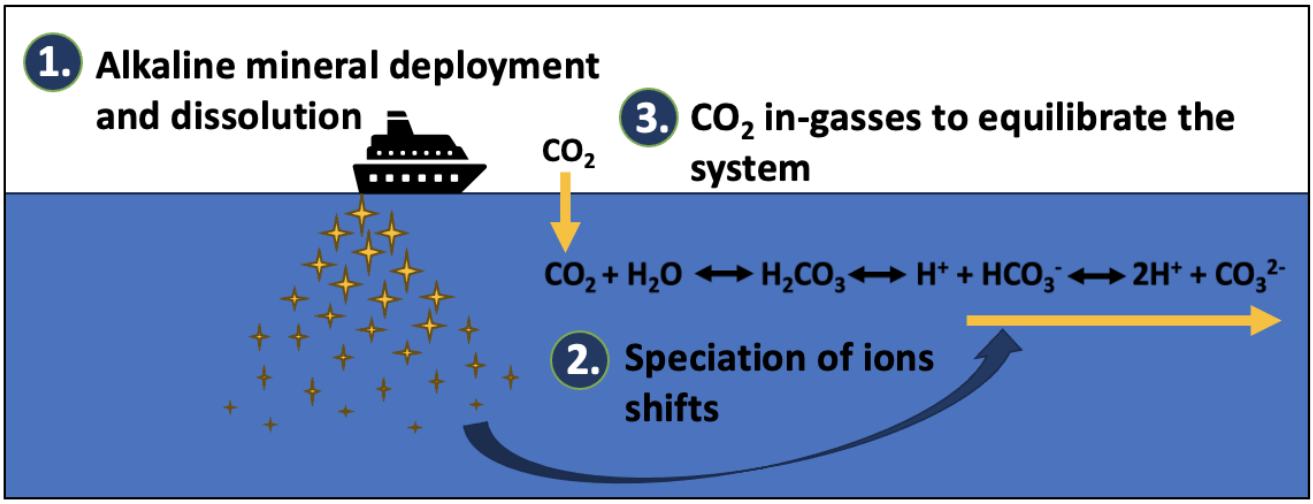

Figure 1. Physical and chemical processes of alkalinization and CO_2 removal by OAE displayed as steps 1-3.

In recent years, much of the conversation of CDR has shifted to include marine CDR, given the large capacity of the ocean to store CO_2 and the overwhelming consensus that multiple CDR approaches will be necessary to reach optimal CO_2 removal capacity (Smith *et al*., 2024). Ocean Alkalinity Enhancement (OAE), also referred to as enhanced weathering, is an emerging marine-based CDR method that is inspired by the natural silicate and carbonate weathering feedback. The overall goal of OAE is to enhance the rate at which the CO_2 moves from the atmosphere into the ocean. In the context of CO_2 drawdown, ocean alkalinity can be considered the ocean's capacity to absorb and store atmospheric CO_2. OAE utilizes the acid-base chemistry of the marine carbonate system to increase the ocean's capacity to absorb and store atmospheric CO_2 through the addition of alkaline solutions at the surface ocean. Alkalinity addition will increase the buffering capacity of the seawater, converting aqueous CO_2 to stable bicarbonate and carbonate ions as the speciation

of dissolved inorganic carbon (DIC) ions shifts, reducing the concentration of bicarbonate (HCO_3^-) ions and increasing the concentration of carbonate (CO_3^{2-}) ions. The resultant surface ocean CO_2 deficit is then equilibrated by the in-gassing of atmospheric CO_2 (Figure 1).

While this process is often referred to as enhanced weathering, it is not to be confused with enhanced rock weathering and does not involve the physical weathering of rocks. Rather, it utilizes alkaline solutions and to simulate Earth's silicate and carbonate chemical weathering feedback in response to increasing atmospheric CO_2–a feedback that typically operates on 10,000-100,000 year timescales (Berner *et al*., 1983). This natural chemical weathering process is responsible for the sequestration of ~0.5 Gt of CO_2 yr^{-1} (Renforth and Henderson, 2017), sequestering CO_2 in the form of stable HCO_3^- and CO_3^{2-} ions. OAE aims to accelerate this process using geoengineering approaches, enhancing the rate to one that can offset anthropogenic emissions. Various studies theorize that OAE has the potential for net removal to reach 3 to 30 Gt of CO_2 yr^{-1} (Feng *et al*., 2017; *Renforth and Henderson*, 2017) when utilized to full capacity. Additionally, OAE could temporarily relieve local ocean acidification in areas of deployment.

Despite being considered to have high theoretical feasibility, critical knowledge gaps persist surrounding the potential impacts of OAE on marine organisms. To assess the biological viability of OAE, it is necessary to understand its potential impact on marine organisms, specifically regarding the rapid shifts in pH and alkalinity from the initial deployment of high-alkaline additions to the surface ocean. Phytoplankton have emerged as organisms of interest due to their carbon fixation capabilities as major primary producers and their sensitivity to shifts in environmental systems. Additionally, their foundational role in global marine food webs make them key organisms in ecosystems. Previous studies have recorded diverse results regarding phytoplankton acclimation as response varies between functional group (ie., coccolithophores, diatoms, dinoflagellates) and alkalinity addition type. Multiple studies have recorded a decline in photosynthetic efficiency across monospecific cultures of coccolithophores and diatoms (Gately *et al*., 2023; Oberlander *et al*., 2025) and within community assemblages (Ferderer *et al*., 2022; Guo *et al*., 2024; Ramírez *et al*., 2024). Guo et al. (2025) identified alkalinity type-dependent differential responses in planktonic community composition under steel-slag (CaO-dominant), olivine (Mg_2SiO_4), and sodium hydroxide (NaOH) additions, observing NaOH to have the highest

CO_2 drawdown and the most acute effects on community health. Gately et al. (2023) and Ferderer et al. (2022) observed reduced silicic acid drawdown, reflecting a greater adverse effect of increased alkalinity on diatom populations compared to other phytoplankton functional groups. A study by Faucher et al. (2025) found increasing alkalinity through NaOH addition led to significantly reduced growth rates and lower particulate organic carbon (POC) production in the coccolithophore *Emiliania huxleyi*. These results contradict Gately et al. (2023), who reported no observable effect of either growth rates or POC production in *E. huxleyi* with a limestone-inspired (Na_2CO_3 + $CaCl_2H_4O_2$) addition at similar TA increases over the same period of time.

In addition to their contribution to primary production, coccolithophores play a critical ecological role as a prominent marine calcifier. Coccolithophores account for up to 20% of the planktonic carbon fixation in open ocean regions and contribute ~50% of biogenic calcium carbonate ($CaCO_3$) exported to depth (*Broeker and Clark*, 2009). As the predominant calcifying organism in the surface ocean, coccolithophores are of particular interest in the context of OAE as increased cellular calcification would decrease alkalinity and release CO_2, potentially counteracting the CO_2 removal by OAE. The biomineralization of their $CaCO_3$ shells occurs intracellularly within the coccolith vesicle via the reaction of calcium (Ca^{2+}) and CO_3^{2-} ions (Equation 1). CO_3^{2-} ions do not pass through the plasma membrane, causing calcification to depend on the uptake of HCO_3^-. The H^+ ion is cleaved from HCO_3^-, then released outside the cell. The additional H^+ reacts with existing HCO_3^- and CO_3^{2-} in the seawater, leading to the formation of CO_2 (Figure 2). Monospecific culture laboratory experiments testing the impact of increased alkalinity on coccolithophore calcification led to varying results. Gately et al. (2023) and Faucher et al. (2025) reported a neutral impact on calcification, whereas Riebesell et al. (2000), an ocean acidification paper mimicking pre-industrial seawater CO_2 concentrations with NaOH, reported increased calcification.

Equation 1. $2HCO_3^- + Ca^{2+} \rightarrow CaCO_3 + CO_2 + H_2O$

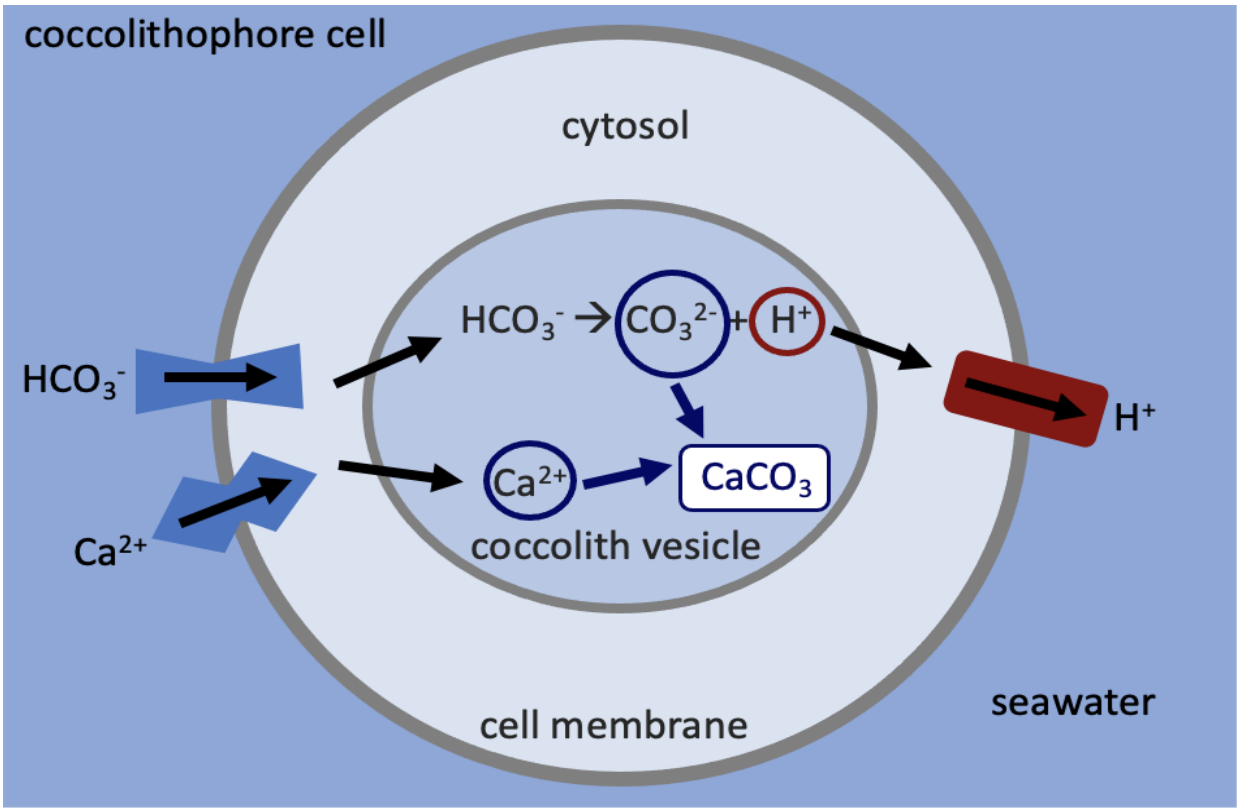

Figure 2. Coccolithophore cellular calcification process, producing calcite ($CaCO_3$) inside the coccolith vesicle and releasing H^+ outside of cell.

While calcification has been studied extensively, there is no conclusive hypothesis for why calcification occurs as it is exhibits high energy demands and strong ballasting effect from the high density of $CaCO_3$ (Monteiro *et al*., 2016). It has been suggested these organisms initially evolved calcifying mechanisms to reduce grazing pressures, however this is still largely debated in literature. Rather, it is suggested that calcification varies across species and strains (Langer *et al*., 2009) and is sensitive to changing environmental conditions (Zondervan *et al*., 2007). This poses coccolithophores as foundational organisms in understanding marine carbon cycling, particularly in comparing inorganic to organic carbon. The particulate inorganic carbon to particulate organic carbon (PIC:POC) ratio is often used as a proxy to couple calcification and photosynthetic rates, determining these processes to either act as a source (>1, conservatively) or sink (<1, conservatively) of CO_2. Variability across studies exists in the PIC:POC ratio, with factors such as light (Zondervan *et al*., 2007) and alkalinity (Findlay *et al*., 2011) exhibiting controls on PIC:POC trends. The effects of increasing CO_2, however, is largely inconclusive as some studies report little to no change in the PIC:POC in the presence of increased CO_2

(Iglesias-Rodriguez *et al*., 2008) while other report considerable differences (Zondervan *et al*., 2007).

Various alkalinity additions have been studied, with the most prominent being NaOH (Faucher *et al*., 2025; Ferderer *et al*., 2022; Guo *et al*., 2025; Oberlander *et al*., 2025), olivine (Guo *et al*., 2025; Guo *et al*., 2024), and carbonate-based (Ferderer *et al*., 2022; Gately *et al*., 2023; Ramírez *et al*., 2024; Subhas *et al*., 2022) however other alkaline solutions are still being considered [ie., steel slag (Guo *et al*., 2024; Guo *et al*., 2025)]. Brucite, a mineral form of $Mg(OH)_2$, has been identified as a potential alkalinity addition due to its abundance in terrestrial environments and prominence as a byproduct of industrial processes (Simandl *et al*., 2007). Existing $Mg(OH)_2$ studies have focused on chemical processes such as CDR potential (Hartmann *et al*., 2023, Yang *et al*., 2023) and precipitation (Shaw *et al*., 2025), or are based in earth system modeling (Anderson *et al*., 2025). Few studies have utilized laboratory experiments to examine the biological impacts of using a magnesium-based alkalinity. Notably, Delacroix et al., (2024) is the only existing study to examine the effect of $Mg(OH)_2$ on microalgae community assemblages. Their results suggest low toxicity effect by $Mg(OH)_2$ in comparison to $Ca(OH)_2$, assessed via survival and growth rates. However, current literature suggests high magnesium seawater is associated with low coccolithophore calcification (Herfort *et al*., 2004, Müller *et al*., 2011) and coccolith malformation (Stanley *et al*., 2005).

In this study, I use a brucite-inspired alkalinity addition (BIAA) to investigate the effects of a high magnesium alkalinity on the growth and calcification of a monospecific *Emiliania huxleyi* cell strain beginning in the stationary cell growth phase through exponential cell growth phase. This is assessed with a laboratory experiment, the data from which I will use to (1) assess the mechanistic role of magnesium in the biogeochemical and physiological processes of *E. huxleyi*, (2) characterize cellular dynamics and response to OAE, and (3) expand the current body of knowledge of OAE investigations evaluating the biological impacts on *E. huxleyi*.

2. Methods

2.1 Experimental Design

A laboratory experiment, in adherence to Iglesias Rodriguez et al. (2023), was conducted over the course of nine days with four sampling time points (Days 0, 3, 6, and 8), with the intention of capturing the exponential growth phase of *E. huxleyi*. The experiment utilized twelve 9 L polycarbonate carboys; six with no alkalinity addition (Controls) and six containing the BIAA. Each group consisted of abiotic and biotic triplicates (Figure 3).

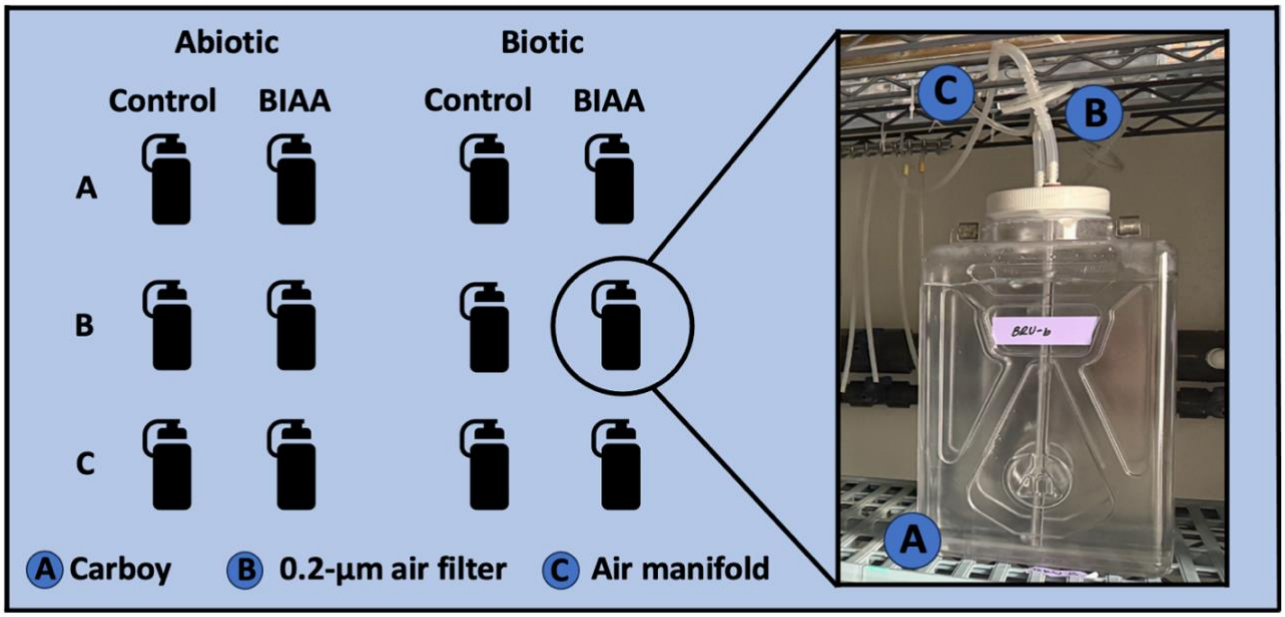

Figure 3. Twelve 9 L polycarbonate carboys; six Control and six BIAA. Each group consisted of abiotic (no cells) and biotic (with cells) triplicates. Image is of experimental carboy and letters are as follows: A. 9 L polycarbonate carboy, B. 0.2-µm polycarbonate air filter, C. Air manifold connected to 420 ppm CO_2 Airgas tank.

Natural seawater was collected from the Santa Barbara Basin and filtered through a 0.22-µm sterile polyethersulfone Steritop filter (Millipore). 8 L of filtered seawater were aliquoted into each acid-rinsed 9 L polycarbonate carboy. An additional twelve acid-rinsed 2 L polycarbonate carboys were utilized for Day 0 technical replicates. All carboys were stored overnight (~12 hours) in the dark at room temperature. The following morning, each carboy was enriched with 100 µM nitrate, 6.24 µM phosphate, and f/2 concentrations of vitamins and trace metals (Langer *et al.*, 2006). Due to incomplete dissolution of $Mg(OH)_2$, we did not use the mineral form of brucite. Instead, we simulated a brucite alkalinity addition using calculated amounts of $MgCl_2*6H_2O$ and NaOH. TA was raised to ~2900 µmol kg^{-1} to mimic a moderate-TA treatment as described in Gately et al.

(2023) based on model predictions (*Renforth and Henderson*, 2017). Biotic carboys were inoculated with monospecific cultures of *E. huxleyi* (morphotype A. over-calcified from June 2015, collected by the Iglesias-Rodriguez lab from the Santa Barbara Basin) with ~2000 cells per ml.

Throughout the course of the experiment, carboys were kept at 15 °C under cool fluorescent light (photon flux density ~190 µmol m^{-2} s^{-1}; 16/8-hour light/dark cycle) and were gently bubbled (~1 bubble/second) with 420 (± 2%) parts per million by volume CO_2 (Airgas) to mimic modern surface ocean gas exchange. Ventilation caps were secured with Parafilm and connected to an air manifold with silicone tubing. Autoclaved 0.2-µm polycarbonate air filters (Omicron) were placed upstream of the ventilation ports to prevent seawater media contamination. Prior to each sampling day, labware was acid-rinsed and autoclaved for sterility. Sample collection began immediately after cell inoculation (Day 0). 2 L of sample media were aliquoted into a 2 L polycarbonate bottle for further allocation of media to minimize carboy disconnection time from manifold (~7 min). To minimize potential variability due to the photocycle, sampling was initiated at 10:00 am (± 30 min) PT on each designated sampling day.

2.2 Sample Analyses

2.2.1 Carbonate Chemistry

Samples were collected in a 250 ml borosilicate bottle, allowing sample media to overflow for half the amount of time to fill the bottle and pouring at an angle to prevent introducing bubbles. Samples were preserved with 100 µl of $HgCl_2$ using a 200 µl serological pipette, sealed with Apiezon L vacuum grease, and stored at room temperature. Prior to analysis, samples were filtered through a syringe using a 0.2-µm filter (Whatman). Total alkalinity (TA) was analyzed with a Mettler Toledo T5 titrator using the open-cell titration protocols outlined by Dickson et al., 2007. Salinity was measured with a YSI 3100 conductivity probe. pH was analyzed using a Shimadzu UV-1280 spectrophotometer and calibrated m-cresol purple dye (*Clayton and Byrne*, 1993). Using measurements of TA, pH, salinity, temperature, and dissolved inorganic nutrients, the remaining carbonate chemistry variables were calculated with CO2sys (Lewis *et al*., 1998) using refit equilibrium constants from Mehrbach et al. (1973) and the total pH scale.

2.2.2 Particulate Inorganic Carbon

200 ml of sample media were vacuum-filtered (<10 Hg) through a 0.2-µm polycarbonate filter on a 47 mm filter funnel into a 1 L side-arm Erlenmeyer flask. The 0.2-µm filter was placed in a 50 ml tube (Falcon) and stored at -20 °C until analysis. All filters were acidified with 0.1 M HNO_3^- following methods outlined in Matson et al. (2019). Cellular particulate inorganic carbon (PIC) values were normalized using *E. huxleyi* cell abundances. Particulate calcium and sodium ion concentrations were analyzed via inductively coupled plasma optical-emission spectrometry [Perkin-Elmer Optima 7300DV] at the University of California, Riverside, Environmental Sciences Research Laboratory.

2.2.3 Particulate Organic Carbon and Particulate Organic Nitrogen

200 ml of sample media were vacuum-filtered (<10 Hg) through a pre-combusted 25 mm GF/F filter. The sample filter was stored at -20°C before analysis via automated organic element analysis using the dumas combustion method [CEC 440HA, Exeter Analytical]. Cellular particulate organic carbon (POC) and particulate organic nitrogen (PON) values were normalized using *E. huxleyi* cell abundances. Analysis was conducted by the University of California, Santa Barbara, Marine Science Institute Analytical Lab.

2.2.4 Dissolved Inorganic Nutrients

~50 mL of filtered sample media was transferred to a 60 mL HDPE bottle and stored at -20 °C until analysis. Nitrate + nitrite (DIN), phosphate (DIP), and silicate (DSi) were measured via flow injection analysis [Seal Analytical continuous-flow AutoAnalyzer 3 (AA3)]. Analysis was conducted by the University of California, San Diego, Scripps Institute of Oceanography, Oceanographic Data Facility.

2.2.5 Microscopy

2 ml of sample media were aliquoted into a 5 ml cryogenic vial using a 1000 µl serological pipette. Samples were preserved with 20 µl of 25% glutaraldehyde fixative solution using a 50 µl serological pipette 0.25% and stored at 4°C. *E. huxleyi* cell abundances (cells per ml) were estimated with an Olympus BX53 light microscope and a 1 mL Sedgewick Rafter counting chamber.

2.2.6 Statistical Analysis

Growth rates (μ, days $^{-1}$) and generation times (days) were determined by applying a linear regression model to the natural logarithm-transformed cell abundances per unit time. A Wilcoxon rank-sum test was performed on biological parameters which includes POC, PON, PIC, PIC:POC, and POC:PON.

3. Results

3.1 Seawater Carbonate Chemistry

The introduction of BIAA resulted in changes in the carbonate system. In abiotic treatments, BIAA-treated carboys yielded a 27% increase in TA, rising from 2200 μmol kg^{-1} (Control) to 2890 μmol kg^{-1} (Figure 3A)–-a net increase of 690 μmol kg^{-1}. By Day 8, BIAA and Control were comparable to their Day 0 values (<5% difference). pH was increased to 8.81 (± 0) by approximately 0.86 logarithmic units on Day 0, followed by a gradual decline to 8.41 (± 0.14) on Day 8, while Control pH marginally increased (Figure 3B). Partial pressure of CO_2 (pCO_2) was initially decreased by 175% in BIAA, but then rose steadily over the course of the experiment. Comparatively, Control decreased by 24% over the same period (Figure 3C). Total dissolved inorganic carbon (TCO_2) concentrations were initially equal across treatments, but in BIAA it gradually increased by 11%, while TCO_2 in the Control was comparable (<5% difference) (Figure 3D) through the duration of the experiment. Increases in BIAA [TCO_2] despite large CO_2 reductions were likely driven by shifts in the speciation of ions, resulting in a 137% increase in [CO_3^{2-}] (Figure 3F) and a 32% decrease in [HCO_3^-] (Figure 3E).

Between abiotic and biotic carboys, initial (Day 0) carbonate chemistry parameters do not vary outside of the standard deviation of each other; however, biotic treatments report a much larger shift in the carbonate chemistry parameters by Day 8. TA decreased 19% (2400 μmol kg^{-1}) and 17% (1870 μmol kg^{-1}) in BIAA and Control, respectively. Treatments trended similarly, with observable differences beginning on Day 6 (Figure 4A). pH gradually declined from 8.80 (± 0) to 8.57 (± 0.04) in biotic BIAA-treated carboys, yielding a 0.23 logarithmic unit decrease. Biotic Control carboys marginally increased in pH by 0.05 logarithmic units. Abiotic BIAA-treated carboys decreased pH by 0.16 units more than biotic BIAA-treated carboys. BIAA and Control

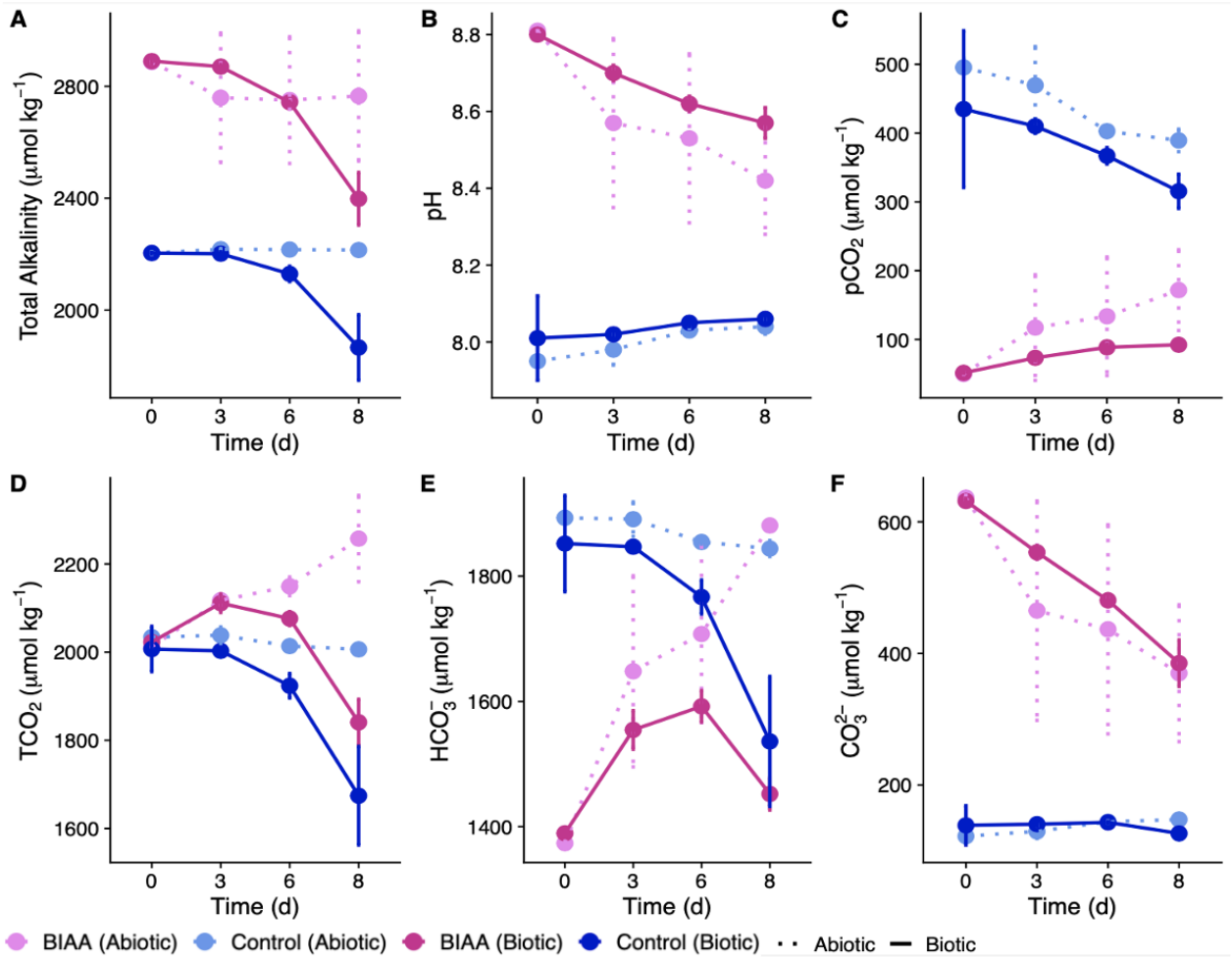

Figure 4. Carbonate chemistry trends over Days 0-8. Color and line type represent treatment (Control; BIAA) and condition (Abiotic; Biotic), respectively. Letters are as follows: A. Total Alkalinity (µmol kg^{-1}), B. pH, C. pCO_2 (µmol kg^{-1}), D. Total CO_2 (TCO_2) (µmol kg^{-1}), E. HCO_3^- (µmol kg^{-1}), F. CO_3^{2-} (µmol kg^{-1}).

exhibited similar trends for pH, with BIAA showing a gradual decrease and Control a gradual increase (Figure 4B). pCO_2 in biotic carboys was lower in both BIAA and Control than in their abiotic counterparts (see figure), reflecting a higher capacity to uptake CO_2 in biotic carboys than in abiotics. pCO_2 increased 57% and decreased 32% in BIAA and Control treatments by Day 8, respectively (Figure 4C).

Between abiotic and biotic treatments, initial TCO_2 concentrations did not differ; however biotic treatments had a net decrease in concentrations. [TCO_2] decreased by 9 and 18% in BIAA and Control treatments, respectively. The initial biotic BIAA trend matched abiotic BIAA, increasing

from Day 0 to Day 3. Biotic Control trended similarly to abiotic Control, seeing little to no effect on TCO_2 between Days 0 and 3. By Day 6 onwards, [TCO_2] was decreasing in both Control and BIAA treatments compared to their abiotic counterparts (Figure 4D). Similarly, the decrease in [HCO_3^-] lagged in biotic Control while biotic BIAA gradually increased. Notably, [HCO_3^-] in BIAA does not begin to decrease until Day 8, whereas a decrease in Control begins on Day 6. This results in a 4% net [HCO_3^-] increase in BIAA and 19% net [HCO_3^-] decrease in Control treatments by Day 8 (Figure 4E). The concentration of CO_3^{2-}, however, trends quite differently. [CO_3^{2-}] decreased 48% and 9% in BIAA and Control treatments, respectively. The steady removal of CO_3^{2-} ions in BIAA appears linear, whereas concentrations in the Control treatment remained relatively stable throughout the experiment (Figure 4F).

3.2 Dissolved Inorganic Nutrients

Experimental results demonstrated distinct nutrient drawdown patterns between treatments, with dissolved inorganic phosphate (DIP) and dissolved inorganic nitrogen (DIN), in the forms of nitrate and nitrite, removal in both biotic treatments. There was no observed removal of dissolved silica (DSi) throughout the course of the experiment, confirming no contamination by silicifiers (Figure 5C).

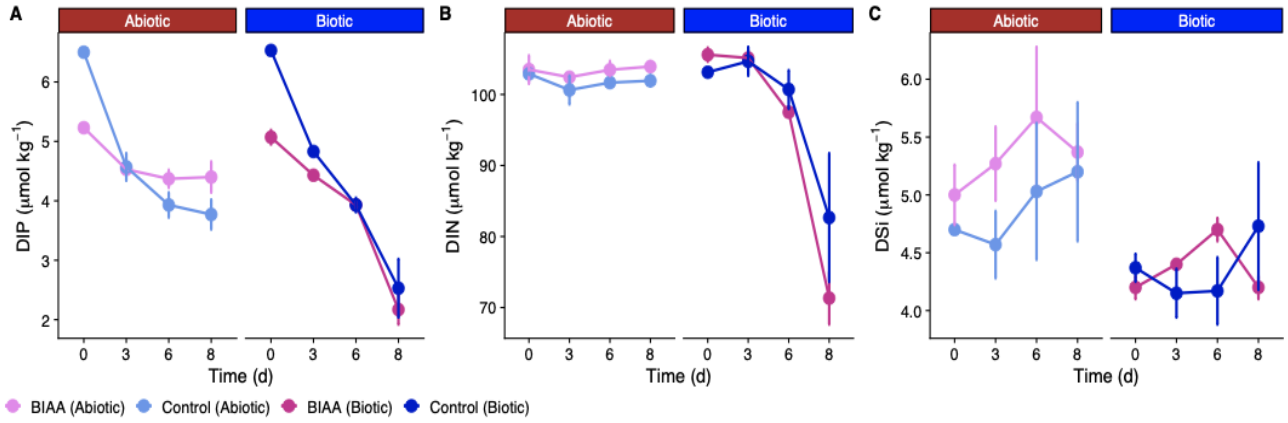

Figure 5. Inorganic nutrient removal over the course of the experiment for dissolved inorganic nutrients. Color represents treatment (Control; BIAA) and condition (Abiotic; Biotic), respectively.

In the biotic treatments, the extent of removal differed slightly between treatments as BIAA consistently showed higher cumulative nutrient removal in DIN and DIP. However, the reported values were within the standard deviation between treatment types due to the high degree of

variability across replicates. Immediate removal of DIP resulted in a 25% difference between treatment types on Day 0, with BIAA resulting in faster initial DIP removal compared to Control. By Day 6, there was no difference in [DIP] between treatment types, but on Day 8 [DIP] was 15% lower in BIAA than in control (Figure 5A). During the exponential phase (Days 6-8), DIN removal accelerated significantly. We observed comparable (<5% difference) in DIN between BIAA and Control treatments on Day 0; however, higher removal of DIN by BIAA was observed by Day 8 (15%) (Figure 5B). Throughout the experiment, DIP and DIN remained replete while DSi remained depleted.

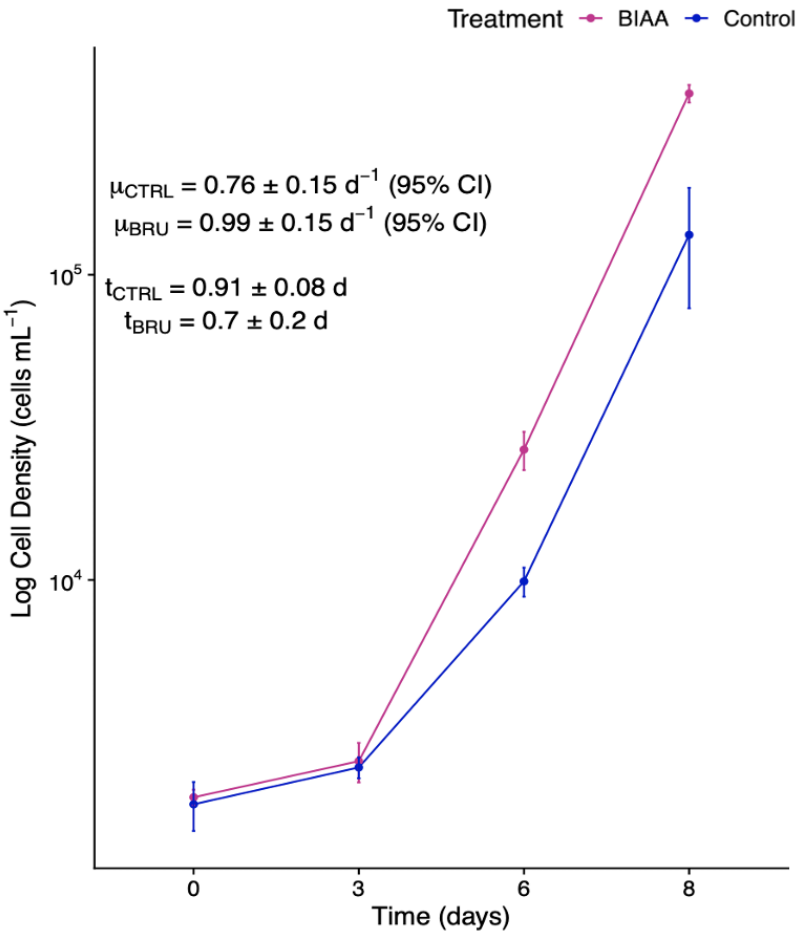

Figure 6. Cell abundance trends over Days 0-8. Color corresponds to treatment (Control; BIAA). Growth rates (μ, days $^{-1}$) and generation times (days) were determined by applying a linear regression model to logarithm-transformed cell abundances per unit time.

In the abiotic treatments, we only observed removal in DIP over time. Immediate removal of DIP resulted in a 22% difference between treatment types on Day 0. This difference decreased to 9% on Day 3, before increasing to 15% on Day 8. Abiotic DIP removal trended similarly to biotic DIP removal (Figure 5A). There was no observed removal in abiotic DIN or DSi.

3.3 Physiological and biogeochemical responses of *E. huxleyi*

We observed the specific growth rates (μ, $days^{-1}$) and generation times (days) of *E. huxleyi* to be increased in BIAA compared to Control. A lag in growth is observed in Days 0-3 (Figure 6). A Wilcoxon rank-sum test was applied to cellular particulate inorganic carbon (PIC) ($W = 59$, $p = 0.1135$),

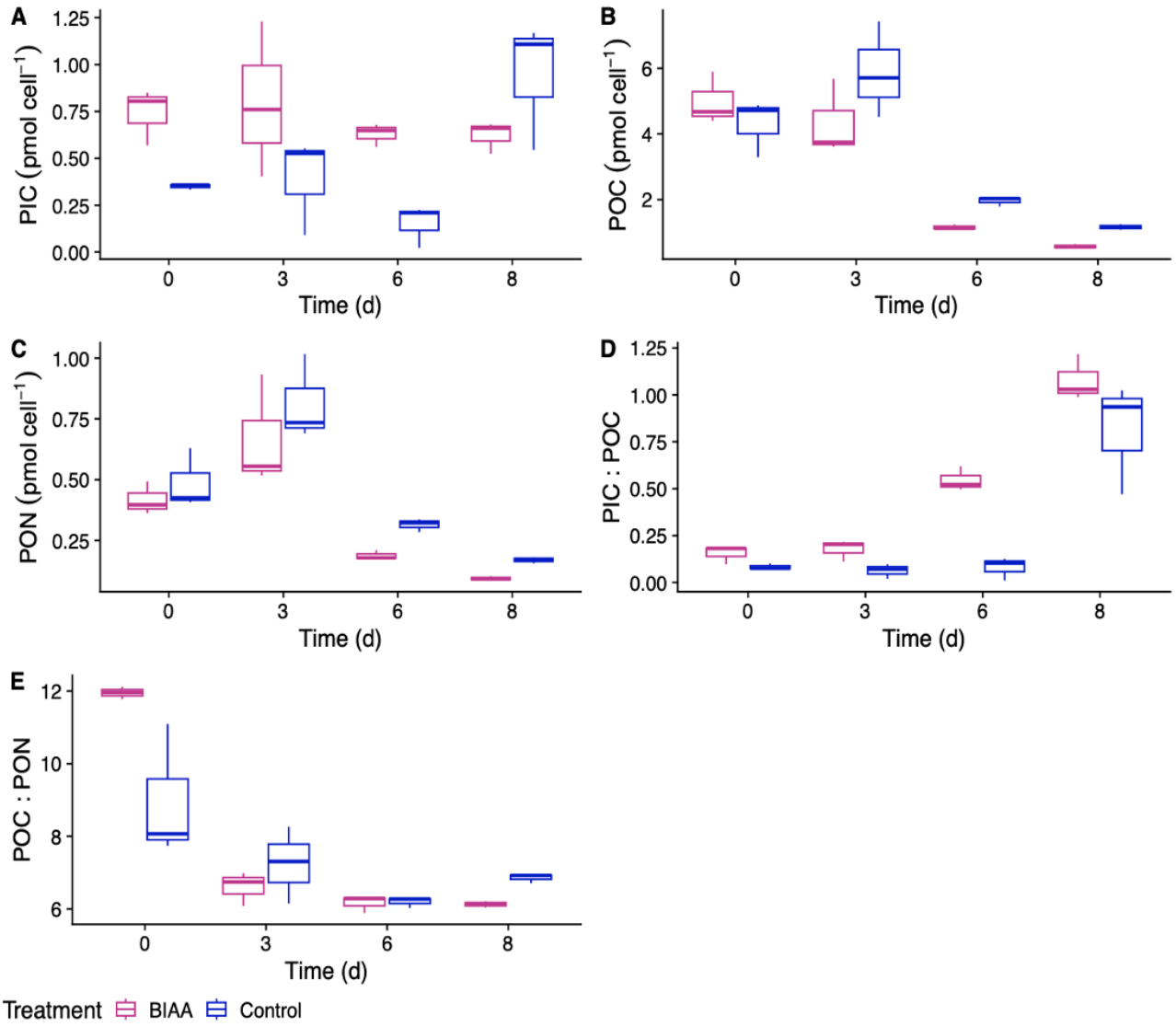

Figure 7. Biogeochemical and physiological processes over Days 0-8. Color represents treatment (Control; BIAA). A Wilcoxon rank-sum test was performed to compare the medians of BIAA and Control; PIC (picomole cell^{-1}) ($W = 59$, $p = 0.1135$), POC (picomole cell^{-1}) ($W = 23$, $p = 0.1359$), PON (picomole cell^{-1}) ($W = 27$, $p = 0.2581$), and POC:PON ($W = 25$, $p = 0.1903$) were not found to have significantly different medians. PIC:POC was found to have significantly different medians ($W = 64$, $p = 0.03998$).

cellular POC ($W = 23$, $p = 0.1359$), cellular particulate organic nitrogen (PON) ($W = 27$, $p = 0.2581$), PIC:POC ($W = 64$, $p = 0.03998$), and POC:PON ratios ($W = 25$, $p = 0.1903$), returning no statistically significant results in between treatment groups, with the exception of PIC:POC. Day 0 values were excluded from statistical tests due to the use of technical replicates and lag in cell growth (Figure 7).

4. Discussion

We observe an increase in *E. huxleyi* growth rates under BIAA treatments compared to the Control. Our results are in direct contrast with previous OAE studies using monospecific coccolithophore cultures. Gately et al. (2023) observed no change in growth rates using a carbonate-based alkalinity addition, while Faucher et al. (2025) reported a decline in growth rates using NaOH. This suggests that $MgCl_2*6H_2O$ utilized in addition to NaOH to mimic $Mg(OH)_2$ could be causing this increase in growth. Magnesium, an essential macronutrient used in the chloroplast for photosynthesis, is typically replete in seawater and not considered a limiting nutrient for growth. However, a study by Müller et al. (2011) observed the response of *E. huxleyi* to changing seawater Mg/Ca ratios and reported an insignificant yet observable increase in growth rates when cells were grown in magnesium-rich seawater, and a significant decrease in growth rates with magnesium depletion. Their results imply a correlation between growth rates and magnesium concentrations, suggesting that the $MgCl_2*6H_2O$ compound used in our alkalinity addition is the cause of the observed increase in growth rates within the BIAA treatment.

Our biogeochemical and physiological analyses suggest that cell size was decreasing over the course of the experiment. This was indicated by the high volume of cellular POC present at the start of the experiment and its subsequent downward sloping trend over time. This trend is observed in both POC and PON values, as well as reflected in the POC:PON ratio. Such changes can be attributed to a range of environmental factors [ie., nutrient limitation, CO_2 concentrations, and temperature (*Aloisi*, 2015)]. It is possible that a decrease in cell size reflects acclimation to the experimental conditions in the carboys, however it remains unclear as to what parameter or combination of parameters may be responsible for the observed changes across both Control and BIAA treatments. Notably, the BIAA treatment exhibited a more pronounced decline in POC compared to the Control, suggesting smaller cell sizes under enhanced alkalinity. Current research indicates that coccolithophore cell size tends to increase with rising atmospheric CO_2 concentrations (*Aloisi*, 2015; *Henderiks and Pagani*, 2008; Iglesias-Rodriguez *et al*., 2008). This implies that we might observe the opposite effect of smaller cell sizes when enhanced alkalinity temporarily reduces CO_2 levels in seawater. Additionally, the enhanced growth rates observed under BIAA treatment may be associated with increased metabolic activity as smaller cells are generally more metabolically active (*Aloisi*, 2015).

Our cell abundances suggest that the cells experience a delayed exponential growth phase, characterized by minimal growth between Days 0 and 3 which is then followed by a sharp increase in cell abundance between Days 3 and 6. This lag in cell growth at the start of the experiment is reflected across multiple parameters, with a strong signal appearing in the carbonate chemistry data. Notably, TA shows a more pronounced decline in the biotic carboys compared to the abiotic carboys, driven by biogenic calcification utilizing HCO_3^- ions and shifting the relative concentrations of DIC species that determine TA in solution. Similar trends were observed with pH as biotic BIAA carboys exhibited a slower decline in pH over the course of the experiment, suggesting that photosynthetic activity by *E. huxleyi* removed aqueous CO_2 and partially offset the acidification caused by the CO_2 bubbling system. Removal of aqueous CO_2 by photosynthetic activity is similarly observed in TCO_2 and pCO_2 as well. The lag in HCO_3^- to respond to biological activity indicates a potential shift towards CO_2 utilization as the primary carbon source rather than HCO_3^- in photosynthetic processes. CO_3^{2-} ion concentrations exhibited a relatively linear decrease over time, largely influenced by the CO_2 bubbling system. The abiotic carboys showed substantial variability in CO_3^{2-} concentrations, likely due to a lack of biological buffering and inconsistencies in the bubbling system across carboys introduced.

A lack of statistical difference between Control and BIAA in PIC (pmol $cell^{-1}$) suggests calcification, while slightly variable between treatments, was relatively stable and unaffected by BIAA. However, the PIC:POC ratio was significantly different ($W= 64$, $p = 0.03998$) between treatments. As this ratio serves to determine whether calcifying phytoplankton are a source (conservatively, >1) or sink (conservatively, <1) of CO_2, PIC:POC can inform interpretations of cell growth stage and seawater carbonate chemistry. While the decrease in cell size and resultant decreasing POC trends are likely responsible for the temporal increase in PIC:POC, the difference between the treatments remains significant as POC (pmol $cell^{-1}$) was observed to be lower in cellular concentrations in BIAA compared to Control. While this difference was not determined to be statistically significant ($W = 23$, $p = 0.1359$), it provides context for the treatment-specific significance in PIC:POC. Additionally, PIC:POC reached above values of 1 (0.99-1.21) in BIAA, indicating calcification was a possible source of CO_2 by Day 8. In the context of OAE, this could reduce the capacity of BIAA to remove CO_2. Our results are not consistent with other OAE experiments using monospecific cultures of *E. huxleyi* (Gately *et al*., 2023, Faucher *et al*., 2025), highlighting the differential effects of BIAA on cell physiology compared to other alkalinity

additions. A study by Riebesell et al. (2000), however, reported increased PIC:POC under enhanced alkalinity using NaOH. All three studies, in addition to our study, increase TA to similar concentrations (~2900-3000 umol kg^{-1}) by an alkalinity addition; yet, the results of each study are varied, suggesting the DIC species shift with alkalinity enhancement might not the driving factor in determining PIC:POC. These studies are in contrast with ours, reporting calcification as the driver in affecting PIC:POC rather than POC production as our results suggest. It is possible species strain-specific adaptations (Langer *et al*., 2009) or alkalinity addition composition could play a role in POC production, as is previously suggested in the discussion. These specifications could be responsible for the variability observed across studies, indicating the potential nuances regarding POC production under a magnesium-rich alkalinity addition.

We observed the accumulation of an orange precipitate across all carboys over the course of the experiment, potentially coinciding with DIP removal in the inorganic nutrient stock (Figure 5A). Precipitation in BIAA carboys was observed to be more pronounced than in Control carboys, however this observation is not sustained in the resultant DIP concentrations as Day 8 reflects similar removal of DIP across both BIAA and Control treatments. This suggests that other dissolved replete constituents, such as iron, may have been removed as well. Precipitate analysis was not performed for this experiment; however, its likely composition is supported by SEM-EDX data reported by Gately et al. (2023). Their findings identified precipitates containing phosphorus and iron, consistent with the formation of iron-phosphates or iron-oxides. Furthermore, Gately et al. (2023) observed similar DIP trends and alkalinity addition concentrations in their abiotic carboys when compared to our study, suggesting the potential role of alkalinity in regulating DIP removal by way of precipitation. Previous work has shown that phosphate can precipitate out of seawater in association with magnesium (Golubev *et al*., 2001), providing further support for the correlation of DIP removal and precipitate formation. Finally, the absence of removal in both DSi and DIN in abiotic carboys confirms all biology larger than 0.2-µm was removed during filtration, suggesting biological contamination is unlikely the cause of DIP removal in our abiotic carboys. The broader implications of inorganic nutrient removal lie in overall nutrient availability. Our results imply OAE has the potential to precipitate nutrients from seawater and reduce nutrient availability, which could affect primary productivity. While our results do not find primary productivity to be reduced under BIAA, our cultures were replete in nutrients and were not likely

affected by nutrient removal. However, this is unlikely to be the case in a naturally variable marine environment where nutrients are often limiting.

This experiment is a part of a broader study investigating the role of magnesium in the use of brucite treatments for OAE. We have demonstrated that our brucite-inspired treatment influences both growth and calcification; however, additional data is required to definitively state and elucidate the underlying mechanisms. Future experimentation should aim to incorporate measurements of seawater and PIC Mg/Ca ratios, as well as coccolith morphology imagery via scanning electron microscopy with energy-dispersive x-ray (SEM-EDX). SEM-EDX analysis of the formed precipitates would confirm their composition and enhance our understanding of precipitate occurrences under OAE. Furthermore, assessing photosynthetic efficiency under BIAA may provide valuable insight into cellular responses and function to a magnesium-rich alkalinity addition, while also providing comparisons across OAE studies, such as those conducted by Gately et al. (2023) and Oberlander et al. (2025).

5. Conclusion

In this study, our aim was to assess the effects of using a magnesium-rich alkalinity enhancement on the growth and calcification on *E. huxleyi*. To achieve this, we performed a laboratory mesocosm experiment, raising TA to ~2900 µmol kg^{-1} using a brucite-inspired alkalinity composed of $MgCl_2*6H_2O$ and NaOH, referred to as BIAA. Notably, BIAA treatments promoted increased growth rates of *E. huxleyi* relative to the Control. The observed enhancement in growth may be attributed to the presence of $MgCl_2*6H_2O$ in BIAA, suggesting a physiological response to increased magnesium availability. Furthermore, the pronounced decline of cellular POC in BIAA suggests BIAA cells were smaller than those in Control. This could be attributed to a decrease in seawater [CO_2]. Enhanced nutrient removal in addition to delayed reductions in TA and pH in biotic BIAA carboys support the hypothesis of enhanced growth as it highlights the role of biology in regulating abiotic processes. Calcification, measured using PIC (pmol $cell^{-1}$), was determined to be consistent across treatments; however, a significant increase in the PIC:POC ratio was observed under BIAA. This indicates calcification may be outpacing photosynthesis, which could have implications for carbon sequestration and OAE efficiency. Furthermore, the

accumulation of the orange precipitate suggests increased alkalinity through OAE has the potential to remove inorganic nutrients from solution.

These results indicate that BIAA caused multiple impacts across biogeochemical and physiological processes. Our study emphasizes the variability across OAE experiments and reinforces the need to expand the current body of literature to understand the dynamics between alkalinity and biological response. While laboratory results are essential indicators to determine species baseline resilience, it is important to note that these experiments do not simulate natural environments and cannot be representative of environmental impacts. They can, however, inform future experimentation and field-trials, lending a hand to future research within the field.

6. References

Aloisi, G. (2015). Covariation of metabolic rates and cell size in coccolithophores. *Biogeosciences*, *12*(15), 4665–4692. https://doi.org/10.5194/bg-12-4665-2015

A Research Strategy for Ocean-based Carbon Dioxide Removal and Sequestration. (2022). Washington, D.C.: National Academies Press. https://doi.org/10.17226/26278

Anderson, H. J., Mongin, M., & Matear, R. J. (2025). Ocean alkalinity enhancement in a coastal channel: simulating localised dispersion, carbon sequestration and ecosystem impact. *Environmental Research Communications*, *7*(4), 041012. https://doi.org/10.1088/2515-7620/adce5a

Berner, R. A., Lasaga, A. C., & Garrels, R. M. (1983). Carbonate-silicate geochemical cycle and its effect on atmospheric carbon dioxide over the past 100 million years. *Am. J. Sci.; (United States)*, *283:7*. https://doi.org/10.2475/ajs.283.7.641

Broecker, W., & Clark, E. (2009). Ratio of coccolith CaCO3 to foraminifera CaCO3 in late Holocene deep sea sediments. *Paleoceanography*, *24*(3). https://doi.org/10.1029/2009PA001731

Clayton, T. D., & Byrne, R. H. (1993). Spectrophotometric seawater pH measurements: total hydrogen ion concentration scale calibration of *m*-cresol purple and at-sea results. *Deep Sea Research Part I: Oceanographic Research Papers*, *40*(10), 2115–2129. https://doi.org/10.1016/0967-0637(93)90048-8

Delacroix, S., Nystuen, T. J., Tobiesen, A. E. D., King, A. L., & Höglund, E. (2024). Ocean alkalinity enhancement impacts: regrowth of marine microalgae in alkaline mineral concentrations simulating the initial concentrations after ship-based dispersions. *Biogeosciences*, *21*(16), 3677–3690. https://doi.org/10.5194/bg-21-3677-2024

Dickson, A. G., Sabine, C. L., Christian, J. R., Bargeron, C. P., & North Pacific Marine Science Organization (Eds.). (2007). *Guide to best practices for ocean CO2 measurements*. Sidney, BC: North Pacific Marine Science Organization.

Faucher, G., Haunost, M., Paul, A. J., Tietz, A. U. C., & Riebesell, U. (2025). Growth response of *Emiliania huxleyi* to ocean alkalinity enhancement. *Biogeosciences*, *22*(2), 405–415. https://doi.org/10.5194/bg-22-405-2025

Feng, E. Y., Koeve, W., Keller, D. P., & Oschlies, A. (2017). Model-Based Assessment of the CO2 Sequestration Potential of Coastal Ocean Alkalinization. *Earth's Future*, *5*(12), 1252–1266. https://doi.org/10.1002/2017EF000659

Ferderer, A., Chase, Z., Kennedy, F., Schulz, K. G., & Bach, L. T. (2022). Assessing the influence of ocean alkalinity enhancement on a coastal phytoplankton community. *Biogeosciences*, *19*(23), 5375–5399. https://doi.org/10.5194/bg-19-5375-2022

Findlay, H. S., Calosi, P., & Crawfurd, K. (2011). Determinants of the PIC : POC response in the coccolithophore Emiliania huxleyi under future ocean acidification scenarios. *Limnology and Oceanography*, *56*(3), 1168–1178. https://doi.org/10.4319/lo.2011.56.3.1168

Friedlingstein, P., O'Sullivan, M., Jones, M. W., Andrew, R. M., Bakker, D. C. E., Hauck, J., et al. (2023). Global Carbon Budget 2023. *Earth System Science Data*, *15*(12), 5301–5369. https://doi.org/10.5194/essd-15-5301-2023

Gately, J. A., Kim, S. M., Jin, B., Brzezinski, M. A., & Iglesias-Rodriguez, M. D. (2023). Coccolithophores and diatoms resilient to ocean alkalinity enhancement: A glimpse of hope? *Science Advances*, *9*(24), eadg6066. https://doi.org/10.1126/sciadv.adg6066

Golubev, S. V., Pokrovsky, O. S., & Savenko, V. S. (2001). Homogeneous precipitation of magnesium phosphates from seawater solutions. *Journal of Crystal Growth*, *223*(4), 550–556. https://doi.org/10.1016/S0022-0248(01)00681-9

Guo, J. A., Strzepek, R. F., Swadling, K. M., Townsend, A. T., & Bach, L. T. (2024). Influence of ocean alkalinity enhancement with olivine or steel slag on a coastal plankton community in Tasmania. *Biogeosciences*, *21*(9), 2335–2354. https://doi.org/10.5194/bg-21-2335-2024

Guo, J. A., Strzepek, R. F., Yuan, Z., Swadling, K. M., Townsend, A. T., Achterberg, E. P., et al. (2025). Effects of ocean alkalinity enhancement on plankton in the Equatorial Pacific. *Communications Earth & Environment*, *6*(1), 1–8. https://doi.org/10.1038/s43247-025-02248-7

Hartmann, J., Suitner, N., Lim, C., Schneider, J., Marín-Samper, L., Arístegui, J., et al. (2023). Stability of alkalinity in ocean alkalinity enhancement (OAE) approaches – consequences for durability of CO_2 storage. *Biogeosciences*, *20*(4), 781–802. https://doi.org/10.5194/bg-20-781-2023

Henderiks, J., & Pagani, M. (2008). Coccolithophore cell size and the Paleogene decline in atmospheric CO2. *Earth and Planetary Science Letters*, *269*(3), 576–584. https://doi.org/10.1016/j.epsl.2008.03.016

Herfort, L., Loste, E., Meldrum, F., & Thake, B. (2004). Structural and physiological effects of calcium and magnesium in *Emiliania huxleyi* (Lohmann) Hay and Mohler. *Journal of Structural Biology*, *148*(3), 307–314. https://doi.org/10.1016/j.jsb.2004.07.005

Iglesias-Rodriguez, M. D., Halloran, P. R., Rickaby, R. E. M., Hall, I. R., Colmenero-Hidalgo, E., Gittins, J. R., et al. (2008). Phytoplankton Calcification in a High-CO2 World. *Science*, *320*(5874), 336–340. https://doi.org/10.1126/science.1154122

Iglesias-Rodríguez, M. D., Rickaby, R. E. M., Singh, A., & Gately, J. A. (2023). Laboratory experiments in ocean alkalinity enhancement research. *State of the Planet*, *2-oae2023*, 1–18. https://doi.org/10.5194/sp-2-oae2023-5-2023

Langer, G., Geisen, M., Baumann, K.-H., Kläs, J., Riebesell, U., Thoms, S., & Young, J. R. (2006). Species-specific responses of calcifying algae to changing seawater carbonate chemistry. *Geochemistry, Geophysics, Geosystems*, *7*(9). https://doi.org/10.1029/2005GC001227

Lewis, E, et al. "Program developed for CO2 system calculations." , Feb. 1998. https://doi.org/10.2172/639712.

Matson, P. G., Washburn, L., Fields, E. A., Gotschalk, C., Ladd, T. M., Siegel, D. A., et al. (2019). Formation, Development, and Propagation of a Rare Coastal Coccolithophore Bloom. *Journal of Geophysical Research: Oceans*, *124*(5), 3298–3316. https://doi.org/10.1029/2019JC015072

Mehrbach, C., Culberson, C. H., Hawley, J. E., & Pytkowicx, R. M. (1973). Measurement of the Apparent Dissociation Constants of Carbonic Acid in Seawater at Atmospheric Pressure. *Limnology and Oceanography*, *18*(6), 897–907. https://doi.org/10.4319/lo.1973.18.6.0897

Müller, M. N., Lebrato, M., Riebesell, U., Barcelos e Ramos, J., Schulz, K. G., Blanco-Ameijeiras, S., et al. (2014). Influence of temperature and CO_2 on the strontium and magnesium composition of coccolithophore calcite. *Biogeosciences*, *11*(4), 1065–1075. https://doi.org/10.5194/bg-11-1065-2014

Oberlander, J. L., Burke, M. E., London, C. A., & MacIntyre, H. L. (2025). Assessing the impacts of simulated ocean alkalinity enhancement on viability and growth of nearshore species of phytoplankton. *Biogeosciences*, *22*(2), 499–512. https://doi.org/10.5194/bg-22-499-2025

Ramírez, L., Pozzo-Pirotta, L. J., Trebec, A., Manzanares-Vázquez, V., Díez, J. L., Arístegui, J., et al. (2025). Ocean alkalinity enhancement (OAE) does not cause cellular stress in a phytoplankton community of the subtropical Atlantic Ocean. *Biogeosciences*, *22*(7), 1865–1886. https://doi.org/10.5194/bg-22-1865-2025

Renforth, P., & Henderson, G. (2017). Assessing ocean alkalinity for carbon sequestration. *Reviews of Geophysics*, *55*(3), 636–674. https://doi.org/10.1002/2016RG000533

Riebesell, U., Zondervan, I., Rost, B., Tortell, P. D., Zeebe, R. E., & Morel, F. M. M. (2000). Reduced calcification of marine plankton in response to increased atmospheric CO2. *Nature*, *407*(6802), 364–367. https://doi.org/10.1038/35030078

Shaw, C., Ringham, M. C., Carter, B. R., Tyka, M. D., & Eisaman, M. (n.d.). Using Magnesium Hydroxide for Ocean Alkalinity Enhancement: Elucidating the Role of Formation Conditions on Material Properties and Dissolution Kinetics. Retrieved from https://www.authorea.com/doi/full/10.22541/essoar.174526332.27681207?commit=011684c6dd41e2f36708166ba42ef7da43027249

Simandl, G., Paradis, S., & Irvine, M. (2007). Brucite – Industrial Mineral with a Future. *Geoscience Canada*, *34*(2), 57–64.

Smith, S. M., Geden, O., Gidden, M. J., Lamb, W. F., Nemet, G. F., Minx, J. C., Buck, H., Burke, J., Cox, E., Edwards, M. R., Fuss, S., Johnstone, I., Müller-Hansen, F., Pongratz, J., Probst, B. S., Roe, S., Schenuit, F., Schulte, I., Vaughan, N. E. (eds.) The State of Carbon Dioxide Removal 2024 - 2nd Edition. https://www.stateofcdr.org DOI 10.17605/OSF.IO/F85QJ (2024).

Stanley, S. M., Ries, J. B., & Hardie, L. A. (2005). Seawater chemistry, coccolithophore population growth, and the origin of Cretaceous chalk. *Geology*, *33*(7), 593–596. https://doi.org/10.1130/G21405.1

Subhas, A. V., Marx, L., Reynolds, S., Flohr, A., Mawji, E. W., Brown, P. J., & Cael, B. B. (2022). Microbial ecosystem responses to alkalinity enhancement in the North Atlantic Subtropical Gyre. *Frontiers in Climate*, *4*. https://doi.org/10.3389/fclim.2022.784997

UNFCCC, “Adoption of the Paris Agreement” (FCCC/CP/2015/L.9/Rev.1, 2015).

Yang, B., Leonard, J., & Langdon, C. (2023). Seawater alkalinity enhancement with magnesium hydroxide and its implication for carbon dioxide removal. *Marine Chemistry*, *253*, 104251. https://doi.org/10.1016/j.marchem.2023.104251

Zondervan, I. (2007). The effects of light, macronutrients, trace metals and CO2 on the production of calcium carbonate and organic carbon in coccolithophores—A review. *Deep Sea Research Part II: Topical Studies in Oceanography*, *54*(5), 521–537. https://doi.org/10.1016/j.dsr2.2006.12.004

Zondervan, I., Rost, B., & Riebesell, U. (2002). Effect of CO_2 concentration on the PIC/POC ratio in the coccolithophore *Emiliania huxleyi* grown under light-limiting conditions and different daylengths. *Journal of Experimental Marine Biology and Ecology*, *272*(1), 55–70. https://doi.org/10.1016/S0022-0981(02)00037-0